

## Optical absorption by free holes in heavily doped GaAs

M. L. Huberman, A. Ksendzov, A. Larsson, R. Terhune, and J. Maserjian

Center for Space Microelectronics Technology, Jet Propulsion Laboratory, California Institute of Technology, Pasadena, California 91109

(Received 23 January 1991; revised manuscript received 4 March 1991)

Optical absorption in *p*-type GaAs with hole concentrations between  $10^{19}$  and  $10^{20}$   $\text{cm}^{-3}$  has been measured for wavelengths between 2 and 20  $\mu\text{m}$  and compared with results of theoretical calculations. In contrast to previous measurements at lower doping levels, the occupied hole states are far from the zone center, where the heavy- and light-hole bands become parallel. This gives rise to a large joint density of states for optical transitions. It is found that the overall magnitude of the observed absorption is explained correctly by the theory, with both free-carrier (indirect) and inter-valence-band (direct) transitions contributing significantly to the total absorption. The strength of the absorption ( $\alpha \approx 20\,000$   $\text{cm}^{-1}$  for  $N_A = 5 \times 10^{19}$   $\text{cm}^{-3}$ ) is attractive for long-wavelength infrared-detector applications.

### I. INTRODUCTION

In this work we investigate both experimentally and theoretically optical absorption by free holes in GaAs for high hole concentrations, a regime which has not been investigated previously. This work is motivated by possible applications in heterojunction internal photoemission, an approach for long-wavelength infrared detection.<sup>1,2</sup>

Previous studies<sup>3,4</sup> of optical absorption in *p*-type GaAs were limited to relatively low hole concentrations  $N_A \leq 10^{18}$   $\text{cm}^{-3}$ . By means of molecular-beam-epitaxial growth, higher hole concentrations between  $10^{19}$  and  $10^{20}$   $\text{cm}^{-3}$  are achievable.<sup>5</sup> Such high concentrations of holes have possible advantages for both inter-valence-band (direct) and free-carrier (indirect) absorption. First, at high doping levels, the heavy-hole band is filled far from the zone center, where the heavy- and light-hole bands become parallel (see Fig. 1). Allowed transitions from the heavy- to light-hole band thus have a large joint density of states. Since the transition rate is proportional to the joint density of states, inter-valence-band absorption is enhanced within a narrow spectral band. (This effect of an increasing joint density of states is partially offset by a decreasing optical matrix element.) Second, since free-carrier absorption is proportional to both carrier concentration and scattering rate,<sup>6</sup> and the scattering rate increases with doping, free-carrier absorption is also enhanced.

At such high carrier concentration one needs to consider the possible limitations caused by plasma reflection, since the plasma frequency then falls in the infrared. For thick layers, light having a wavelength greater than the plasma wavelength is reflected, its absorption thus being reduced; but for the thin layers used in internal photoemission devices (in order to maximize the collection efficiency) this effect is found to be negligible.

### II. EXPERIMENT

The 2.0- $\mu\text{m}$ -thick *p*-type GaAs layers used in this study were grown by molecular-beam epitaxy on Cr-doped

GaAs(100) substrates, following a 0.5- $\mu\text{m}$ -thick undoped GaAs buffer layer. The substrate temperature was kept at 580°C. Beryllium was used as the *p*-dopant and the highest hole concentration achieved under normal growth conditions (growth rate = 1.0  $\mu\text{m}/\text{h}$ ,  $\text{As}_4$  beam pressure equal to  $3 \times 10^{-6}$  Torr) was  $1.5 \times 10^{20}$   $\text{cm}^{-3}$ . At this high doping level the surface morphology degraded, but for the other samples used, having hole concentrations  $4.5 \times 10^{19}$  and  $2.5 \times 10^{19}$   $\text{cm}^{-3}$ , a mirrorlike surface was obtained.

The hole concentrations and mobilities were measured by the standard van der Pauw four-probe technique. For the doping concentrations which were investigated, most of the carriers ( $\sim 90\%$ ) are in the heavy-hole band. We used both a one-band model (heavy holes only) and a two-band model (heavy and light holes with the same

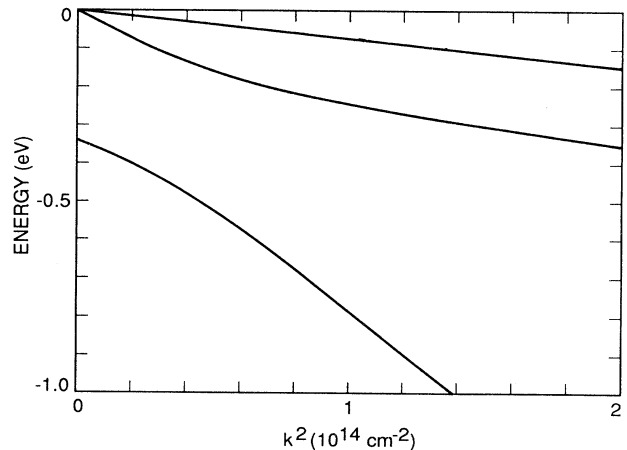


FIG. 1. Valence-band structure of GaAs calculated by  $\mathbf{k} \cdot \mathbf{p}$  theory assuming isotropic energy bands. Heavy-hole mass  $m_{\text{hh}} = -0.50m$ , light-hole mass  $m_{\text{lh}} = -0.088m$ , and spin-orbit splitting  $\Delta = 0.34$  eV. For  $N_A = 5 \times 10^{19}$   $\text{cm}^{-3}$ , the Fermi energy  $E_F = -0.094$  eV.

mean free path) to find the hole concentrations and mobilities from the measured Hall coefficients and resistivities. Since the results for the two models were found to be practically the same, a one-band model is used for simplicity. The hole concentrations and mobilities determined for the three samples which were investigated are then  $N_A = 2.5 \times 10^{19}$ ,  $4.5 \times 10^{19}$ , and  $1.5 \times 10^{20} \text{ cm}^{-3}$ , and  $\mu = 60$ ,  $60$ , and  $50 \text{ cm}^2/\text{Vs}$ , respectively.

To determine the percent absorption of our samples we measured transmission and reflectance (near normal incidence configuration) using a Fourier-transform spectrometer. The measurements were performed at room temperature in the  $2\text{--}28 \mu\text{m}$  spectral range with the light incident on the doped-layer side. To avoid optical losses, the substrate side of the samples was lapped and polished.

### III. THEORY

In order to calculate the power absorbed in a thin layer of  $p$ -type GaAs, we first derive the frequency-dependent conductivity, from which the complex dielectric constant is obtained. Using the dielectric constant, we then solve Maxwell's equations to find the absorbed power.

The total conductivity is the sum of contributions from free-carrier (indirect) transitions and from inter-valence-band (direct) transitions. The free-carrier conductivity is derived by semiclassical transport theory, which in a degenerate semiconductor is expected to be satisfactory, provided that the photon energy  $\hbar\omega$  is not much greater than the Fermi energy  $E_F$ .<sup>7</sup> Using a one-band model, the frequency-dependent conductivity for free carriers is then

$$\sigma_{id}(\omega) = \frac{\sigma_0}{1 - i\omega\tau}, \quad (1)$$

where  $\tau$  is the relaxation time, which is independent of frequency in semiclassical transport theory, and  $\sigma_0$  is the dc conductivity. Using the measured values of the dc mobility  $\mu$  and the relation  $\mu = e\tau/m^*$  where  $m^* = 0.5m$  is the heavy-hole effective mass in GaAs,  $m$  is the free-electron mass, and  $e$  is the magnitude of the electron charge, we find  $\tau = 1.7 \times 10^{-14}$ ,  $1.7 \times 10^{-14}$ , and  $1.4 \times 10^{-14} \text{ s}$  for  $N_A = 2.5 \times 10^{19}$ ,  $4.5 \times 10^{19}$ , and  $1.5 \times 10^{20} \text{ cm}^{-3}$ , respectively.

To find the contribution to the conductivity from inter-valence-band transitions, we first derive an expression for the absorbed power using time-dependent perturbation theory. The conductivity is then found from the expression for the absorbed power using a damped harmonic oscillator model.<sup>8</sup>

Since our main interest is in the long-wavelength infrared ( $\lambda > 8 \mu\text{m}$ ), only transitions between the heavy- and light-hole bands are considered (see Fig. 1). Transitions to the split-off hole band and to higher bands, which fall at short wavelengths outside the range of interest, are ignored. The transition energies and matrix elements are found by second-order degenerate  $\mathbf{k}\cdot\mathbf{p}$  perturbation theory,<sup>9</sup> in which the interaction between the valence bands and all other bands is treated as a perturbation. (In the case of Ge, a more exact calculation<sup>10</sup> shows that the heavy- and light-hole energy bands are described well by this approximate theory.) For simplicity, we approxi-

mate the energy bands and transition rates as isotropic by taking the parameters  $L$ ,  $M$ , and  $N$  in  $\mathbf{k}\cdot\mathbf{p}$  perturbation theory to be related by  $L = M + N$ . Although the warpage of the heavy- and light-hole bands in GaAs is large, the separation between them is approximately isotropic, so that this assumption is not expected to have a large effect.

Accordingly it can be shown that the heavy- and light-hole energy bands are

$$E_1(k) = \frac{\hbar^2 k^2}{2m} + Mk^2, \quad (2)$$

$$E_2(k) = \frac{\hbar^2 k^2}{2m} + \frac{1}{2}[(N + 2M)k^2 - \Delta] + \frac{1}{2}(N^2 k^4 + \frac{2}{3}Nk^2\Delta + \Delta^2)^{1/2}, \quad (3)$$

where  $m$  is the free-electron mass and  $\Delta$  is the spin-orbit splitting. For GaAs,  $\Delta = 0.34 \text{ eV}$ .<sup>11</sup> The parameters  $M$  and  $N$  can be related to the heavy- and light-hole effective masses, which are measured experimentally at the zone center; for GaAs at 300 K,  $m_{hh} = -0.50m$ , and  $m_{lh} = -0.088m$ .<sup>11</sup> Using Eq. (2) and the expansion of Eq. (3) near the zone center yields

$$\frac{\hbar^2}{2m_{hh}} = \frac{\hbar^2}{2m} + M, \quad (4)$$

$$\frac{\hbar^2}{2m_{lh}} = \frac{\hbar^2}{2m} + \frac{2}{3}N + M. \quad (5)$$

Far from the zone center, Eq. (3) converges to

$$E_2(k) \rightarrow -\frac{2}{3}\Delta + \frac{\hbar^2 k^2}{2m} + Mk^2, \quad (6)$$

showing that the heavy- and light-hole bands become parallel with an energy separation  $\frac{2}{3}\Delta$ .

By time-dependent perturbation theory, the power absorbed in a unit volume from an electromagnetic wave  $\mathbf{E}(t) = \mathbf{E} \cos(\omega t)$  due to transitions from the heavy- to light-hole band is

$$P = \frac{1}{\Omega} \sum_{\mathbf{k}} \hbar\omega \left[ \frac{2\pi}{\hbar} \right] \left[ \frac{e\hbar\mathbf{E}}{2m\omega} \right]^2 W_{12} \times \delta(E_1(k) - E_2(k) - \hbar\omega), \quad (7)$$

where  $\Omega$  is the total volume and the sum is over allowed transitions from filled to empty states. (Since finite temperatures effects are small for a degenerate semiconductor, the absorbed power is evaluated for zero temperature.)  $W_{12}$  is defined by summing the square of the optical matrix element over both Kramers degenerate final states and averaging over the direction of  $\mathbf{k}$ . Using  $\mathbf{k}\cdot\mathbf{p}$  perturbation theory,<sup>9</sup>

$$W_{12} = \left[ \frac{m}{\hbar^2} \right]^2 \frac{N^2 k^2}{9} (\sqrt{2}S_{22} + S_{23})^2, \quad (8)$$

$$S_{22} = \frac{h_{23}}{[h_{23}^2 + (E'_2 - h_{22})^2]^{1/2}}, \quad (9)$$

$$S_{23} = \frac{h_{22} - E'_2}{[h_{23}^2 + (E'_2 - h_{22})^2]^{1/2}}, \quad (10)$$

$$h_{23} = -\frac{\sqrt{2}}{3} N k^2, \quad (11)$$

$$h_{22} = (\frac{2}{3} N + M) k^2, \quad (12)$$

$$E'_2 = E_2 - \frac{\hbar^2 k^2}{2m}. \quad (13)$$

We use the damped harmonic oscillator model to introduce lifetime broadening of the transition. Replacing the  $\delta$  function of energy conservation with a Lorentzian yields

$$P = \frac{1}{\Omega} \sum_{\mathbf{k}} \omega_{12} \left[ \frac{2\pi}{\hbar} \right] \left[ \frac{e\hbar E}{2m\omega_{12}} \right]^2 W_{12} \frac{2\Gamma\omega^2/\pi}{(\omega^2 - \omega_{12}^2)^2 + \Gamma^2\omega^2}, \quad (14)$$

where  $\Gamma$  is the full width at half maximum of the transition and  $\omega_{12} = (E_1 - E_2)/\hbar$ . For simplicity, we estimate  $\Gamma$  by  $\Gamma = 1/\tau$  where  $\tau$  is the transport lifetime. Using the damped harmonic oscillator model to relate the conductivity to the absorbed power yields for the frequency-dependent conductivity for inter-valence-band transitions

$$\sigma_d(\omega) = \frac{e^2\tau}{\Omega m} \sum_{\mathbf{k}} f_{12} \frac{\Gamma\omega}{\Gamma\omega - i(\omega^2 - \omega_{12}^2)}, \quad (15)$$

where

$$f_{12} = \left[ \frac{2m}{\hbar^2} \right] (\hbar\omega_{12}) \left[ \frac{\hbar}{m\omega_{12}} \right]^2 W_{12}. \quad (16)$$

Finally, converting the sum over allowed transitions to an integral by introducing the joint density of states (per unit volume) for the heavy- and light-hole bands

$$\rho_{12} = \frac{k^2}{\pi^2 |dE_{12}/dk|}, \quad (17)$$

where  $E_{12} = E_1 - E_2$  is the transition energy, we find

$$\sigma_d(\omega) = \frac{e^2\tau}{m} \int dE_{12} \rho_{12} f_{12} \frac{\Gamma\omega}{\Gamma\omega - i(\omega^2 - \omega_{12}^2)}. \quad (18)$$

The total conductivity due to free-carrier and inter-valence-band absorption is the sum of Eqs. (1) and (18),

$$\sigma = \sigma_{id} + \sigma_d. \quad (19)$$

The complex dielectric constant is then

$$\epsilon(\omega) = \epsilon_0 + \frac{4\pi i\sigma}{\omega}, \quad (20)$$

where  $\epsilon_0 = 13.1$  is the static dielectric constant of GaAs. The solution of Maxwell's equations for the electric and magnetic fields inside the absorbing layer is then

$$\mathbf{E} = \hat{\mathbf{x}} E \exp[i(\pm nqz - \omega t)], \quad (21)$$

$$\mathbf{B} = \pm \hat{\mathbf{y}} n E \exp[i(\pm nqz - \omega t)],$$

where  $n = \sqrt{\epsilon}$  and  $q = \omega/c$ . The absorption in a thin lay-

er on an insulating substrate is derived by considering light incident on the layer from vacuum (as in the experimental measurements) and matching electric and magnetic fields at the interface of the thin layer with vacuum and with the substrate. (Reflection from the backside of the thick substrate is treated by adding intensities, since interference effects arising from this reflection average out due to thickness variations of the substrate.) The absorbed power in the thin layer is then the difference between the incident power and the sum of the reflected and transmitted power.

#### IV. RESULTS

The measured absorption spectra of a 2- $\mu\text{m}$ -thick GaAs layer for the three doping concentrations are shown in Fig. 2. The calculated absorption spectra for the same doping concentrations and layer thickness are shown for comparison in Fig. 3. The theoretical curves are calculated without any free parameters, since the electron relaxation time is determined from the dc mobility.

The theory explains the main features of the observed absorption. (The observed absorption peaks between 2 and 4  $\mu\text{m}$  are caused by transitions from the heavy- and light-hole bands to the split-off hole band, which are not included in the theory.) First the theory explains correctly the overall magnitude of the absorption. Second, the theory explains the position of the absorption edge and its shift to shorter wavelengths as the hole concentration increases. This shift is caused by the increasing energy of heavy- to light-hole band transitions as the heavy-hole band is filled. Third, the theory explains the decreasing absorption at long wavelengths with increasing hole concentration. This decrease is caused by the onset of plasma reflection.

The remaining discrepancy between theory and experiment may be due to the simplifying assumptions of the theory, in particular, the assumption that the energy bands and transition rate are isotropic, that the electron

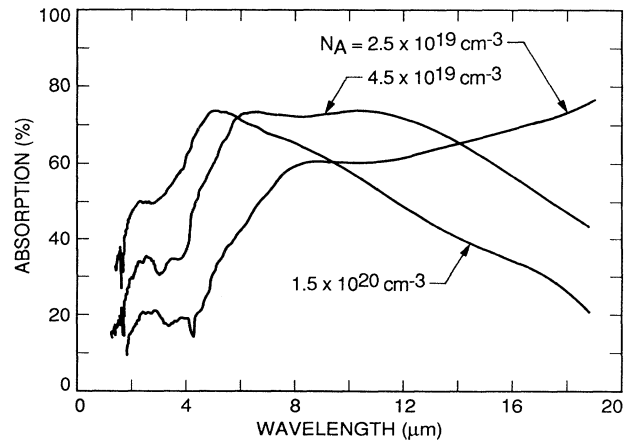


FIG. 2. Experimental absorption spectra of a 2- $\mu\text{m}$  thick *p*-type GaAs layer on a semi-insulating GaAs substrate for light incident on the doped-layer side.

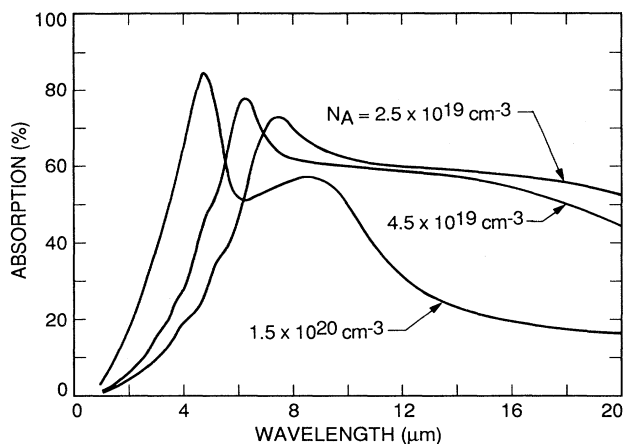


FIG. 3. Theoretical absorption spectra of a 2- $\mu\text{m}$ -thick  $p$ -type GaAs layer on an undoped GaAs substrate for light incident on the doped-layer side.  $\tau = 1.7 \times 10^{-14}$ ,  $1.7 \times 10^{-14}$ , and  $1.4 \times 10^{-14}$  s for  $N_A = 2.5 \times 10^{19}$ ,  $4.5 \times 10^{19}$ , and  $1.5 \times 10^{20}$   $\text{cm}^{-3}$ , respectively.

relaxation time  $\tau$  is independent of frequency, and that the lifetime broadening of the interband transitions  $\Gamma = 1/\tau$  where  $\tau$  is the transport lifetime. The effect of this last assumption is illustrated by the theoretical curves in Fig. 4, in which  $\tau$  is unchanged but the lifetime broadening is increased by a factor of 3. This smooths out the sharp structure in Fig. 3, which does not appear in the experimental data.

For the lowest hole concentration  $N_A = 2.5 \times 10^{19}$   $\text{cm}^{-3}$ , the measured absorption in Fig. 2 continues to increase at longer wavelengths whereas the calculated absorption in Fig. 3 is decreasing. This difference may be due to a breakdown of the isotropic approximation for low hole concentrations. Because the effective masses of the heavy- and light-hole bands are anisotropic, the band filling will also be anisotropic. For high doping, which is our primary interest, when all transitions occur in the re-

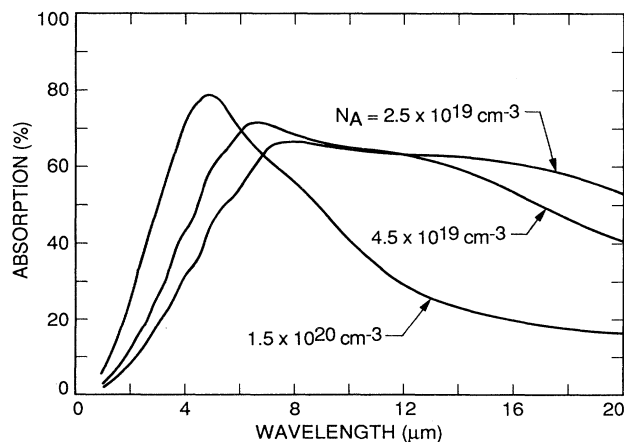


FIG. 4. Theoretical absorption spectra for the same parameters as in Fig. 3, except that the lifetime broadening of the interband transitions  $\Gamma = 3/\tau$  instead of  $\Gamma = 1/\tau$ .

gion of  $\mathbf{k}$  space where the heavy- and light-hole bands are parallel, this will have little effect on the transition energies, since the separation between the heavy- and light-hole bands is approximately isotropic. At low doping, however, the transition energies will depend upon direction in  $\mathbf{k}$  space, leading to increased inter-valence-band absorption at longer wavelengths.

Theoretical absorption spectra for free-carrier absorption alone, inter-valence-band absorption alone, and free-carrier and inter-valence-band absorption together are plotted in Fig. 5 for the hole concentration  $N_A = 4.5 \times 10^{19}$   $\text{cm}^{-3}$ . It is seen that the observed absorption cannot be explained by free-carrier transitions alone, showing that inter-valence-band transitions are important. It is also seen that in such thick layers the total absorption is not just the sum of the absorption for each process alone. This is a result of the interaction of the two processes through the complex dielectric constant.

As an application of this theory, the predicted absorption in a 200- $\text{\AA}$  thick GaAs layer, a thickness which is of interest for heterojunction internal photoemission detectors, is plotted in Fig. 6 for the hole concentration  $N_A = 4.5 \times 10^{19}$   $\text{cm}^{-3}$ . In such thin layers, the total absorption is found to be just the sum of the absorption from each process alone. It is seen that both processes contribute significantly to the total absorption, with inter-valence-band absorption dominating at shorter wavelengths and free-carrier absorption dominating at longer wavelengths. The total absorption in a 200- $\text{\AA}$  layer is found to be approximately constant for  $8 < \lambda < 20$   $\mu\text{m}$ , having the value  $A \approx 4\%$ . In Fig. 7, the total absorption in a 200- $\text{\AA}$  layer is plotted for several hole concentrations, showing its variation with hole concentration.

The absorption coefficient is defined by  $\alpha = 2n''q$ , where  $n''$  is the imaginary part of the index of refraction and  $q = \omega/c$  is the wave number of the light. In Fig. 8, the theoretical absorption coefficient of bulk  $p$ -type GaAs is plotted for several hole concentrations. If reflections

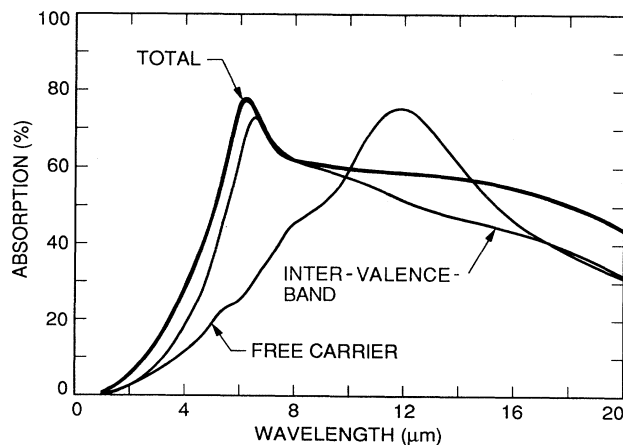


FIG. 5. Theoretical absorption spectra of a 2- $\mu\text{m}$  thick  $p$ -type GaAs layer ( $N_A = 4.5 \times 10^{19}$   $\text{cm}^{-3}$ ) on an undoped GaAs substrate for light incident on the doped-layer side. Free-carrier absorption, inter-valence-band absorption, and total absorption.

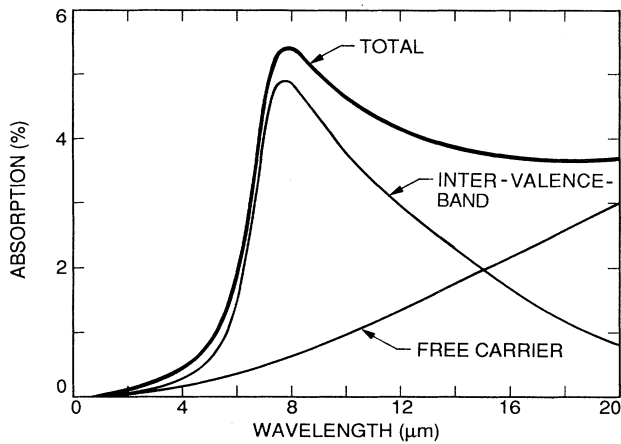


FIG. 6. Theoretical absorption spectra of a 200-Å-thick *p*-type GaAs layer ( $N_A = 4.5 \times 10^{19} \text{ cm}^{-3}$ ) on an undoped GaAs substrate for light incident on the doped-layer side. Free-carrier absorption, inter-valence-band absorption, and total absorption.

can be neglected, the absorption in a layer of thickness  $t$  is related to the absorption coefficient by

$$A = 1 - e^{-\alpha t}, \tag{22}$$

which reduces to  $A = \alpha t$  in the thin-film limit. However, the effect of reflections cannot be neglected even for thin layers. Although for the thin layers in Fig. 7 the absorption is seen to be approximately equal to the product of the absorption coefficient and the layer thickness, this is fortuitous, arising in this geometry from compensating effects of reflections from the front and back surfaces of the wafer. In general, the absorption depends not only on the imaginary part  $n''$  of the refractive index, which is proportional to the absorption coefficient  $\alpha$ , but also on its real part  $n'$ ; and must be found, as has been done here, by matching electric and magnetic fields using the complex refractive index  $n = n' + in''$ , which is plotted in Fig. 9 for completeness.

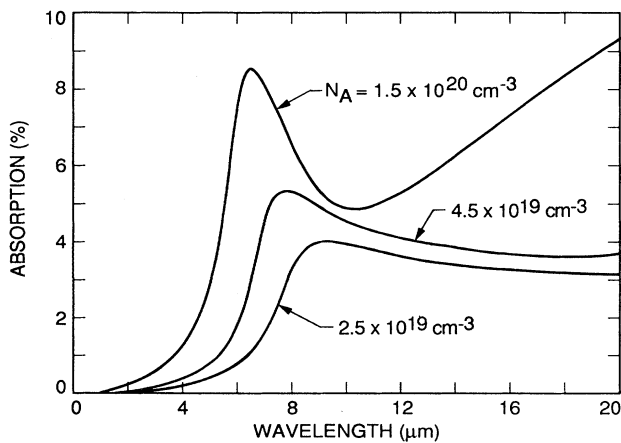


FIG. 7. Theoretical absorption spectra of a 200-Å-thick *p*-type GaAs layer on an undoped GaAs substrate for light incident on the doped-layer side.

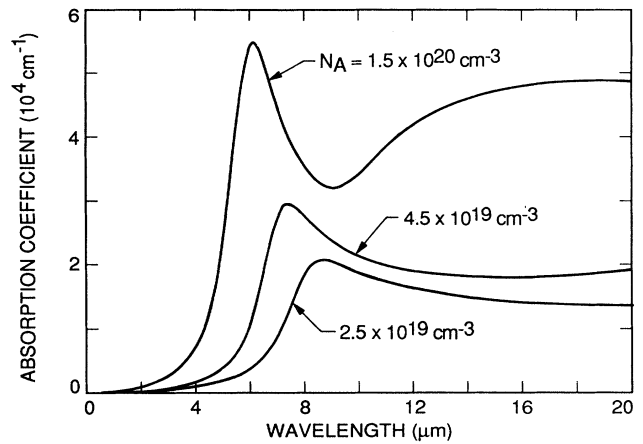


FIG. 8. Theoretical absorption coefficient of bulk *p*-type GaAs.

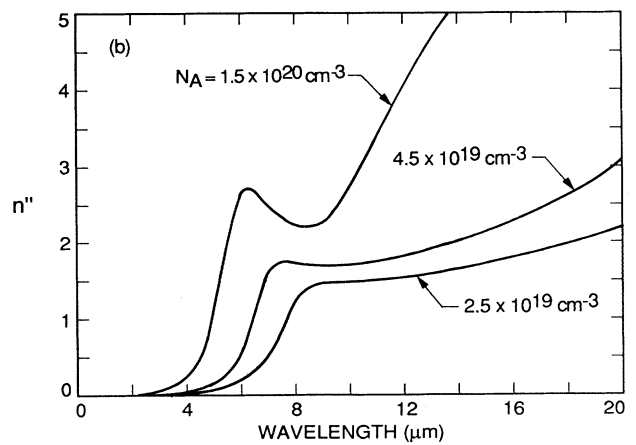
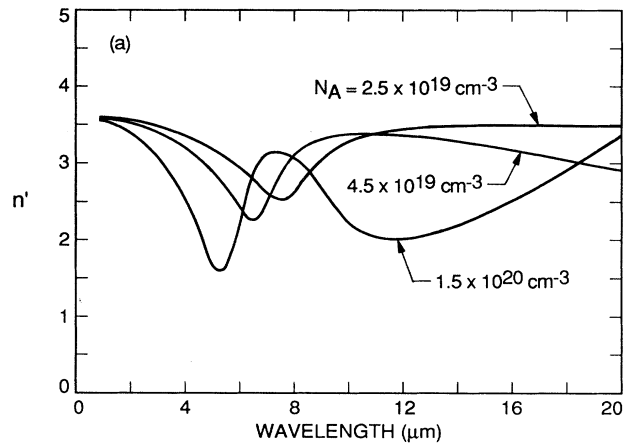


FIG. 9. Theoretical index of refraction of bulk *p*-type GaAs. (a) Real part  $n'$ . (b) Imaginary part  $n''$ .

## V. CONCLUSIONS

It has been shown that the main features of optical absorption in  $p$ -type GaAs at long wavelengths are explained correctly by theory. We have seen that large absorption occurs at high doping due to the contribution of both inter-valence-band (direct) and free-carrier (indirect) absorption. The values of the absorption coefficient are found to be large, e.g.,  $\alpha \approx 20\,000\text{ cm}^{-1}$  for  $N_A = 4.5 \times 10^{19}\text{ cm}^{-3}$ , which has important implications for optical devices. For example, heavily doped  $p^+$  contact layers in long-wavelength detectors (e.g., quantum-well and superlattice III-V detectors) can have a deleterious effect of unwanted absorption. On the other hand, this property is very attractive for heterojunction internal photoemission detectors, where maximum absorption in thin layers is desired.

Although the results have been presented for GaAs, similar considerations apply to related III-V compound and group-IV elemental semiconductors. In the case of Si-Ge alloys, which are also of interest for detector appli-

cations, transitions to the split-off band become important in the long-wavelength regime (8–20  $\mu\text{m}$ ). The theory for inter-valence-band absorption would differ somewhat, but would also be expected to yield strong absorption at high doping. This could be a subject of future work.

## ACKNOWLEDGMENTS

The authors would like to thank Barbara Wilson for support, encouragement, and helpful discussions. This work was done while one of us (M.L.H.) was at the Jet Propulsion Laboratory with financial support from the National Research Council. The work described was performed by the Center of Space Microelectronics Technology, Jet Propulsion Laboratory, California Institute of Technology, and was jointly supported by the Strategic Defense Initiative Organization, Innovative Science and Technology Office, and the National Aeronautics and Space Administration, Office of Aeronautics, Exploration and Technology.

<sup>1</sup>T. L. Lin and J. Maserjian, *Appl. Phys. Lett.* **57**, 1422 (1990).

<sup>2</sup>J. Maserjian, "Heterojunction Internal Photoemission Detectors," Innovative Long Wavelength Infrared Detector Workshop, Jet Propulsion Laboratory, Pasadena, CA, April, 1990, Proceedings published in Publication 90-22 (Jet Propulsion Laboratory, Pasadena, 1990).

<sup>3</sup>R. Braunstein, *J. Phys. Chem. Solids* **8**, 280 (1959).

<sup>4</sup>R. Braunstein and E. O. Kane, *J. Phys. Chem. Solids* **23**, 1423 (1962).

<sup>5</sup>J. L. Lievin and F. Alexandre, *Electron. Lett.* **21**, 413 (1985).

<sup>6</sup>J. I. Pankove, *Optical Processes in Semiconductors* (Prentice-Hall, New Jersey, 1971).

<sup>7</sup>W. P. Dumke, *Phys. Rev.* **124**, 1813 (1961).

<sup>8</sup>For example, see G. Burns, *Solid State Physics* (Academic, New York, 1985).

<sup>9</sup>E. O. Kane, *J. Phys. Chem. Solids* **1**, 82 (1956).

<sup>10</sup>W. Fawcett, *Proc. Phys. Soc. London* **85**, 931 (1965).

<sup>11</sup>J. S. Blakemore, *J. Appl. Phys.* **53**, R123 (1982).